JMEPEG
https://doi.org/10.1007/s11665-019-04202-z

1059-9495/$19.00

Comparison of Experimental Measurements of Thermal Conductivity of Fe_2O_3 Nanofluids Against Standard Theoretical Models and Artificial Neural Network Approach

Ravi Agarwal, Kamalesh Verma, Narendra Kumar Agrawal, and Ramvir Singh

(Submitted December 21, 2018; in revised form June 02, 2019)

In the present work, the practicability of Fe_2O_3 nanofluids for heat transfer applications has been examined. Nanofluids performance, in terms of modulation of thermal conductivity, has been investigated with increasing concentration of Fe_2O_3 nanoparticles in water and ethylene glycol base fluids at 10, 20, 30, 40, 50, 60 and 70 °C. Fe_2O_3 nanoparticles have been synthesized using the wet chemical method and characterized using TEM, SEM, XRD and UV–Vis. The characterization results revealed a face-centered cubic structure having alpha phase and particle size in the range of 40-55 nm for the synthesized Fe_2O_3 nanoparticles. Thermal conductivity measurement results show increases in thermal conductivity with the increase in concentration and temperature of nanofluids. 16.45 and 19.76% enhancement in thermal conductivity have been observed for Fe_2O_3–water and Fe_2O_3–ethylene glycol nanofluids of 2 vol.% at 70 °C compared to water and ethylene glycol base fluids at 10 °C, respectively. Results of the ANN approach are in good agreement with experimental results, and H–C model gives better predictions compared to other standard models. The study gives clear insights into improved heat transfer performance by material engineering.

Keywords heat transfer modulation, nanofluids, neural network, thermal measurement, thermophysical properties

1. Introduction

Heat transfer performance of traditional fluids does not fulfill the needs of current age development. Advanced heat transfer fluids with significantly improved heat transfer characteristics are required for sustainable development. Suspension of metal oxide nanoparticles in fluids exhibits superior thermal properties relative to conventional heat transfer fluids and fluids containing micrometer-/millimeter-sized particles. Thermal conductivity is an important parameter which represents the heat transfer capacity of any thermal system. Many researchers are working to improve thermal conductivity for improved performance.

Hong and Yang (Ref 1) found that Fe nanofluids exhibit more enhancements in thermal conductivity than Cu nanofluids establishing that improvement in thermal transport properties mainly depends on the interaction of nanoparticles with base fluids. Hong et al. (Ref 2) observed nonlinear dependency of thermal conductivity on the volume fraction of the Fe nanofluids that has been attributed to the clustering of nanoparticles in base fluids. Patel et al. (Ref 3) and Eastman et al. (Ref 4) found that the size of nanoparticles matters giving higher thermal conductivity for metal nanoparticles compared to metal oxide nanoparticles. They suggested incorporation of more parameters, viz. size and the effect of stabilizer, for better accuracy of various existing standard models.

According to Wang et al. (Ref 5), the thermal conductivity of nanofluids depends on the microscopic motion of particles in fluids. Development of new models with the inclusion of the microscopic motion may more accurately predict the thermal behavior of nanofluids. The microscopic motion is influenced by size, shape, structure and surface properties of nanoparticles. Experimental results reported by Masuda et al. (Ref 6) and Lee et al. (Ref 7) show that the thermal conductivities of particles and fluids both affect the thermal conductivity of resulting nanofluids. They also suggested a strong dependence of thermal conductivity on the size of the nanoparticles. Murshed et al. (Ref 8) concluded that both particle size and shape influence the thermal conductivity of nanofluids. Thermal conductivity enhancement depends on the stability of the nanofluids suspension that in turn depends on the size, shape and interaction of the nanoparticles. Iijima (Ref 9) and Liu et al. (Ref 10) observed that CNTs having a larger aspect ratio give higher thermal conductivity in their suspensions. In such a case, thermal transport is facilitated by a three-dimensional network of CNTs dispersed in the base fluid.

Along with experimental studies, several theories have also been developed to predict the thermal conductivity of nanofluids. Maxwell (Ref 11), Yu and Choi (Ref 12), Bruggeman (Ref 13) and Hamilton and Crosser (Ref 14) are popular theoretical models that have widely been used for the prediction of the thermal conductivity of the nanofluids (Ref 15-17). Artificial neural network (ANN) has also been implemented to predict the thermophysical properties of nanofluids (Ref 18). The study

Ravi Agarwal, Centre for Converging Technologies, University of Rajasthan, Jaipur 302004, India; **Kamalesh Verma** and **Ramvir Singh**, Department of Physics, University of Rajasthan, Jaipur 302004, India; and **Narendra Kumar Agrawal**, Department of Physics, Poddar International College, Jaipur 302020, India. Contact e-mail: agarwal.ravi.cct@uniraj.ac.in.

Published online: 09 July 2019

by Kurt and Kayfeci (Ref 19) suggested ANN as a practical technique that can help application engineers in predicting thermal conductivity with high accuracy and without exhaustive experiments.

Engineered fluids made up of a combination of different fluids/materials, with controlled volume fractions, can significantly improve the performance of heat transfer systems (Ref 20). A systematic study in this direction is required that can ascertain the effect of change of various parameters, viz. concentration and temperature, on the effective thermal conductivity of nanofluids (Ref 21). Further, combined studies that include theoretical (Ref 22), experimental (Ref 23) and soft computing aspects are scarce (Ref 24). In this study, thermal conductivity behavior of Fe_2O_3–water and Fe_2O_3–ethylene glycol nanofluids has been explored in the temperature range that suits for most real-world applications. Fe_2O_3 nanoparticles have been synthesized using wet chemical method due to widespread applicability to give a size-controlled synthesis of nanoparticles that make the resulting nanofluids cost-effective and tunable. Experimental results have been compared with standard theoretical models and matched with neural network performance (Ref 25).

2. Materials and Methods

Fe_2O_3 nanoparticles have potential applications in many fields of engineering (Ref 26). Fe_2O_3 is of much scientific interest over the other nanoparticle systems due to inherent magnetic properties. Using thermal energy, the magnetic moment can be modulated to give zero net magnetization. Highly sensitive measurements can be performed on samples without further processing, by making a magnetic signal on or off (Ref 27). Magnetic properties of Fe_2O_3 nanoparticles are highly affected by the size, shape, aggregation, etc. So, Fe_2O_3 nanofluids have been investigated in the present study, and the two-step technique has been used for the preparation of nanofluids. Fe_2O_3 nanoparticles have been synthesized using wet chemical method, and synthesized nanoparticles have been used for the preparation of nanofluids in water and ethylene glycol.

2.1 Synthesis and Characterization of Fe_2O_3 Nanoparticles

Fe_2O_3 nanoparticles have been synthesized using the wet chemical method. 0.1 M solution of ferric chloride heptahydrate in water and 0.5 M solution of sodium hydroxide in ethanol have been prepared through continuous stirring for 15 min. These solutions have been simultaneously added in 10 mL water drop by drop through continuous stirring and heating at 80 °C. The solution hence obtained has been further subjected to heat treatment at 100 °C for 15 min. The appearance of dark brown precipitate indicated the formation of Fe_2O_3 nanoparticles. The precipitate has been filtered, washed and dried to obtain nanoparticles in powder form. Synthesized nanoparticles have been characterized using transmission electron microscopy (TEM; Tecnai; FEI G2 S-Twin), scanning electron microscopy (SEM; Carl Zeiss; EVO-18), X-ray diffraction (XRD; PANalytical; X'Pert PRO) and UV–Vis spectrophotometer (UV–Vis; Shimadzu; UV-1800). For characterization, 0.010 g of the synthesized nanoparticles has been dispersed in 10 mL distilled water using vortex (Tarsons; SPINIX). This suspension has been used for TEM, SEM, XRD and UV–Vis analysis.

2.2 Preparation and Thermal Conductivity Measurement of Nanofluids

Specifications of water and ethylene glycol base fluids used in this study are provided in Table 1. For the preparation of 0.25% nanofluids, required amount of Fe_2O_3 nanoparticles (Ref 20) has been weighed (Precisa; XB 220A, 0.0001 g) and mixed in the base fluids (water and ethylene glycol) using a mortar and pestle (Cole-Parmer) to obtain a nanoparticle-based fluid suspension. The suspension has been stirred for an hour by a magnetic stirrer (Tarsons; SPINOT) followed by ultrasonication for 200 min using ultrasonic water bath cleaner (Toshcon, SW4) so as to obtain homogeneously mixed nanofluids. The similar procedure has been adopted to prepare nanofluids of higher concentration (0.5, 0.75, 1, 1.25, 1.5, 1.75 and 2%). Stability of the prepared nanofluids has been monitored for 10 days, and no visible trace of particle sedimentation has been observed.

Thermal conductivity of Fe_2O_3–water and Fe_2O_3–ethylene glycol nanofluids has been measured using KD2 Pro Thermal Properties Analyzer at different temperatures (10, 20, 30, 40, 50, 60 and 70 °C). Experimental setup for thermal conductivity measurement mainly consists of nanofluid sample, sample holder, temperature stabilizing unit and thermal conductivity measuring unit. Figure 1 shows the schematic diagram of the experimental setup used for thermal conductivity measurement. KS-1 sensor (6 cm long and 1.3 mm diameter single needle, accuracy ± 5%) has been used to measure the thermal conductivity of nanofluid samples. The sensor performance has been verified using a standard sample and found to be within 1.05% of the reported value. Refrigerated/heating circulator (MS Julabo; FP-30; ± 0.5 °C) has been used to achieve the desired temperature of nanofluids during measurements. Measurements have been taken using the following steps:

1. Heat or cool the nanofluid sample with the sensor needle inserted in it.
2. Turn the circulator off, once the desired sample temperature has been achieved and equilibrated.
3. Measurements have been taken after the circulator became still. The average of three measurements has been reported.

2.3 Theoretical Models

Experimental results have been compared with predictions of standard theoretical models. Details of the most popularly used models are given below:

Maxwell (Ref 11) proposed the first model which is based on effective medium theory to predict the thermal conductivity of suspensions by assuming that the suspension contains particles of spherical shape and considered only the volume fraction dependency.

$$k_{nf} = \frac{(k_{np} + 2k_{bf}) + 2(k_{np} - k_{bf})\phi}{(k_{np} + 2k_{bf}) - (k_{np} - k_{bf})\phi} k_{bf} \quad \text{(Eq 1)}$$

Table 1 Specifications of base fluids used

Base fluids	Specifications
Distilled water	Producer: ultrapure water (direct Q^R 3 water purification system) Density: 1 g/cm^3 Thermal conductivity: 0.641 W/m K (measured at 30 °C)
Ethylene glycol	Producer: Merck Specialties Private Limited, India Assay: ≥ 99% Density: 1.11 g/cm^3 Thermal conductivity: 0.246 W/m K (measured at 30 °C)

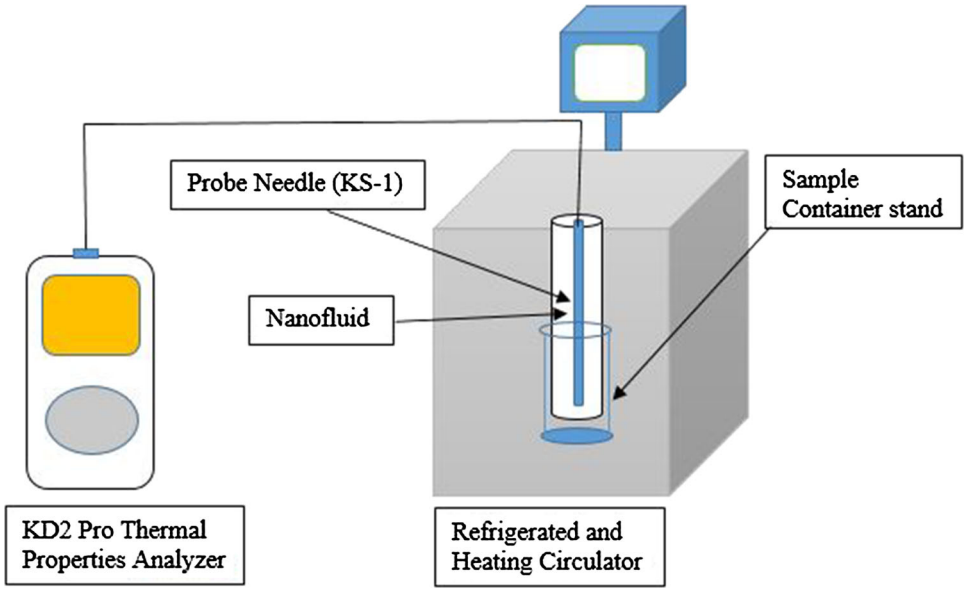

Fig. 1 Experimental setup used for measurement of thermal conductivity of nanofluids

where k_{nf}, k_{np} and k_{bf} represent thermal conductivity of nanofluids, nanoparticles and base fluid, respectively, and ϕ represents volume fraction of nanoparticles.

Yu and Choi (Ref 12) modified Maxwell's model by assuming the formation of an interfacial layer of liquid molecules on the surface of the dispersed nanoparticles.

$$k_{nf} = \frac{\left(k_{np} + 2k_{bf}\right) + 2\left(k_{np} - k_{bf}\right)(1+\gamma)\phi}{\left(k_{np} + 2k_{bf}\right) - \left(k_{np} - k_{bf}\right)(1+\gamma)\phi} k_{bf} \qquad \text{(Eq 2)}$$

where k_{lr} represents the thermal conductivity of the interfacial layer and assumed to be equivalent to the thermal conductivity of nanoparticles. γ is the ratio of the nanoparticle radius (r) to the thickness of one interfacial layer (h) in nm. We considered h = 2 nm in our calculations.

Bruggeman (Ref 13) adopted a mean-field approach to predict the thermal conductivity of nanofluids

$$k_{nf} = \frac{1}{4}\left[(3\phi - 1)k_{np} + (2 - 3\phi)k_{bf}\right] + \frac{k_{bf}}{4}\sqrt{\Delta} \qquad \text{(Eq 3)}$$

$$\text{where } \Delta = \left[(3\phi-1)^2\left(\frac{k_{np}}{k_{bf}}\right)^2 + (2-3\phi)^2 + \left(2+9\phi-9\phi^2\right)\left(\frac{k_{np}}{k_{bf}}\right)\right]$$

Hamilton and Crosser (Ref 14) (H–C) modified Maxwell's model by considering the effect of the particle shape

$$k_{nf} = \frac{k_{np} + (n-1)k_{bf} - (n-1)\phi\left(k_{bf} - k_{np}\right)}{k_{np} + (n-1)k_{bf} + \phi\left(k_{bf} - k_{np}\right)} k_{bf} \qquad \text{(Eq 4)}$$

where $n = \frac{3}{\psi}$, n is a particle shape factor. ψ is the particle sphericity or ratio of the surface area of a sphere (with a volume equal to that of the particle) to the surface area of the particle. ψ is 1 for spherical shape and 0.5 for cylindrical shape. For n = 3 H–C model reduced to Maxwell model. In our calculations, we have taken n = 6 for H–C model.

Verma et al. (Ref 15) predicted the thermal conductivity of nanofluids containing spherical nanoparticles by solving the Laplace equation for the potential with the dispersion of one particle and field is modified at the observation point. A contribution by all the neighboring particles in the modification of field is calculated using summation.

$$k_{nf} = k_{bf}\left[1 + 5.5618\left(\frac{k_{np} - k_{bf}}{k_{np} + 2k_{bf}}\right)F\right] \qquad \text{(Eq 5)}$$

where $F = N\phi$, F represents the correction term for the volume fraction of the filler phase. Value of N is obtained by linear fitting between experimental results and theoretical formulations. Values of the coefficient N obtained were 1.317 and 1.25 for Fe_2O_3–water and Fe_2O_3–ethylene glycol nanofluids, respectively.

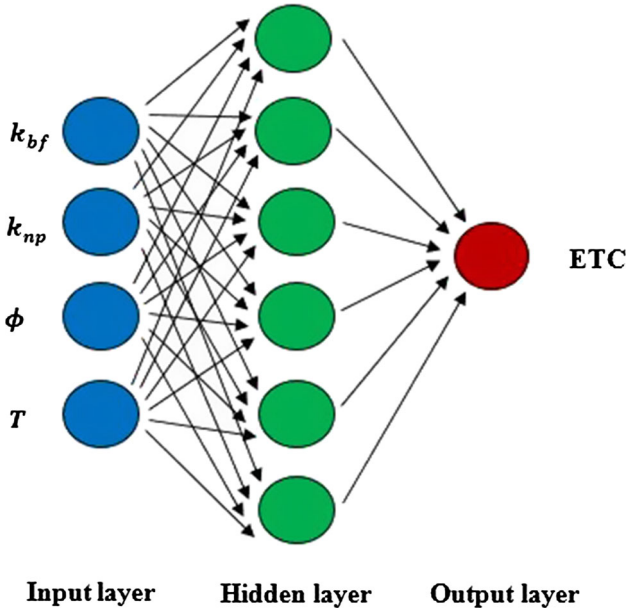

Fig. 2 The architecture of ANN used in our work

2.4 ANN

A comparison of predicted thermal conductivity of nanofluids using ANN approach has also been presented in the paper. Feed-forward back-propagation network architecture with four inputs [thermal conductivity of the base fluid (k_{bf}), the thermal conductivity of the nanoparticles (k_{np}), the volume fraction of the nanoparticles (ϕ) and the temperature of the nanofluid (T)] and one output [thermal conductivity of the nanofluid (k_{nf})] has been used. Figure 2 shows the architecture of ANN used in our work. One hidden layer with varying number of neurons has been tried in the work. The following functions have been adopted in our work:

Training Function—Train LM (Levenberg–Marquart), Adaptive Learning Function—Learn GDM, Transfer Function—TANSIG.

3. Results and Discussion

3.1 Characterization of Fe_2O_3 Nanoparticles

3.1.1 TEM. Shape and particle size distribution of the suspended Fe_2O_3 nanoparticles have been determined using TEM. The sample for TEM analysis has been prepared by placing a few drops of working solution on a carbon-coated standard copper TEM grid (300 mesh). Figure 3(a) shows a TEM image of synthesized Fe_2O_3 nanoparticles that exhibit particle size ranging from 45 to 55 nm. The TEM image gives a perfect view of size, size distribution and morphology. Fe_2O_3 nanoparticles with appropriate boundary can easily be identified in the image having narrow particle size distribution without any agglomeration. Figure 3(b) illustrates selected area electron diffraction (SAED) pattern that identifies the sample based on diffraction from different planes of the sample under investigation. SAED pattern exhibits poly-/nanocrystalline nature of the synthesized nanoparticles based on the Bragg's reflection forming small and bright rings.

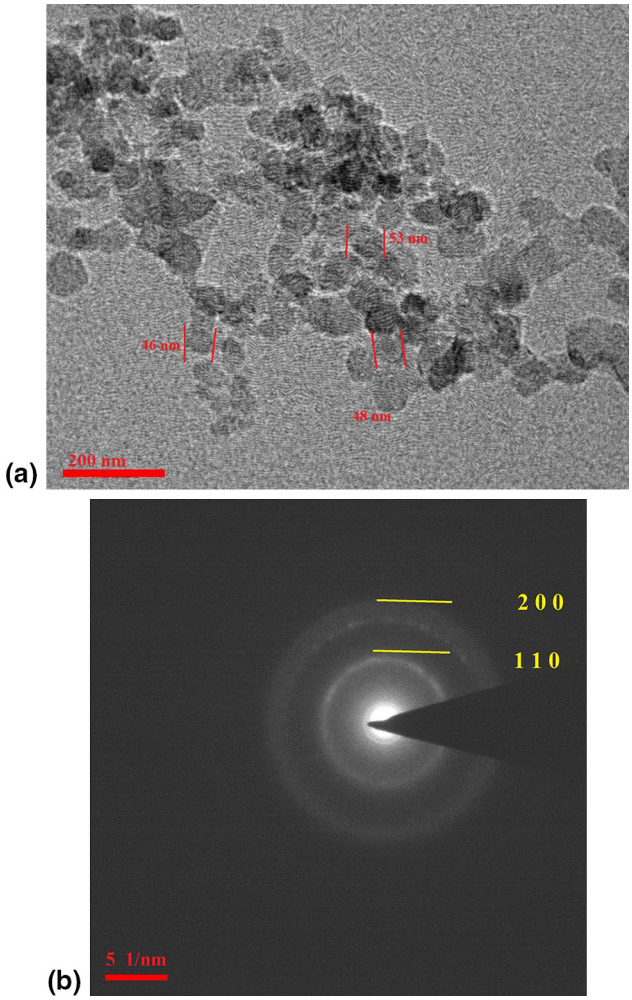

Fig. 3 (a) TEM image of synthesized Fe_2O_3 nanoparticles (b) SAED pattern

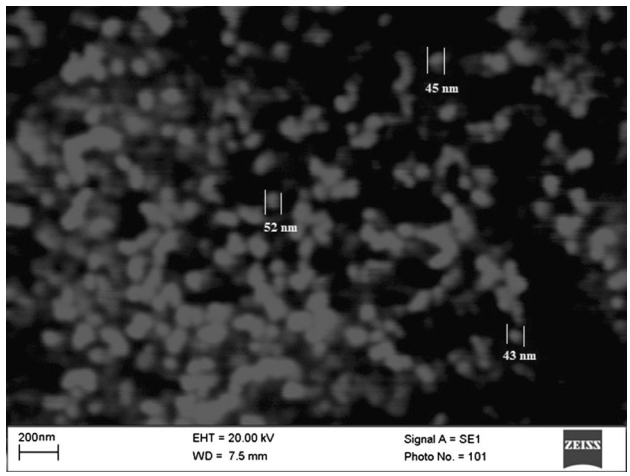

Fig. 4 SEM image of the synthesized Fe_2O_3 nanoparticles

3.1.2 SEM. Particle size in large sample amounts has also been determined using SEM. The sample has been prepared on conducting Si substrates by placing a few drops of working solution on it. Figure 4 shows SEM image of the synthesized Fe_2O_3 nanoparticles. The SEM image exhibits Fe_2O_3 Nanoparticles having a size ranging from 40 to 55 nm.

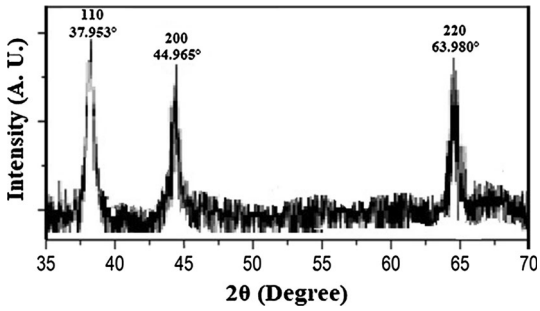

Fig. 5 XRD pattern of the synthesized Fe_2O_3 nanoparticles

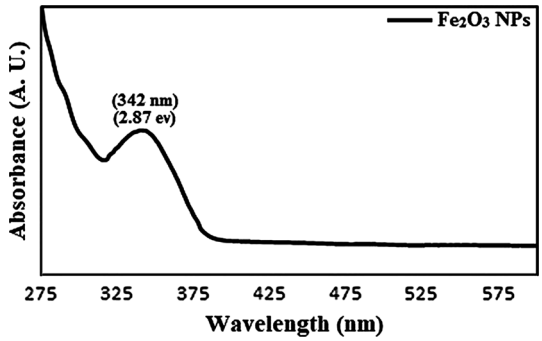

Fig. 6 UV–Vis spectrum of the synthesized Fe_2O_3 nanoparticles

3.1.3 XRD. Phase and particle size determination have also been performed using XRD, in scanning region 2θ from 35° to 70° with a step size = 0.02° and time per step = 1.60 s. Background subtraction, smoothening by Gaussian fitting method and phases identification have been performed through advanced XRD data processing software "Ritward". XRD pattern of the synthesized Fe_2O_3 nanoparticles (Fig. 5) shows typical reflections corresponding to the face-centered cubic structure which is in agreement with published results. The material, phase and structure can be identified by XRD pattern in which diffractions from different planes give diffraction peaks. Here, diffraction peaks are found to be shifted toward lower 2θ values as compared to those of bulk Fe_2O_3. Broad 110, 200 and 220 peaks in XRD spectra have been obtained at 2θ angles 37.953°, 44.965° and 63.980°, respectively, indicating that synthesized Fe_2O_3 nanoparticles are in α phase. The broadening of diffraction peaks in the XRD pattern is ascribed to the nanometer-sized crystallites. The average particle size of the synthesized Fe_2O_3 nanoparticles is 51 nm calculated using the Debye–Scherrer formula.

3.1.4 UV–Vis. Figure 6 shows the absorbance spectrum of the Fe_2O_3 nanoparticles that exhibit typical absorbance at 342 nm corresponding to the interband transition from deep-level electrons of valance band. The band gap of the synthesized Fe_2O_3 nanoparticles is 2.87 eV calculated using *Tauc* relation.

3.2 Thermal Conductivity of Fe_2O_3 Nanofluids

Thermal conductivity of Fe_2O_3 nanofluids has been measured as a function of the concentration of Fe_2O_3 nanoparticles in water and ethylene glycol base fluids ranging from 0.0025 to 0.02 volume fractions at different nanofluids temperatures ranging from 10 to 70 °C. Figure 7 and 8 show measured thermal conductivity of Fe_2O_3–water and Fe_2O_3–ethylene glycol nanofluids, respectively. Thermal conductivity of these nanofluids is higher than that of the base fluids and increases with increasing the volume fraction of the dispersed nanoparticles and/or the temperature of nanofluids. The thermal conductivity increase is higher with the increase in concentration compared to an increase in temperature. Thermal conductivity enhancement with temperature is much more sensitive at higher concentrations. In nanofluids, heat transfer mainly depends on the formation of the layer-like structure between nanoparticles and base fluids (Ref 28). The nanolayer, acting as a bridge, is in an intermediate physical state between liquid and

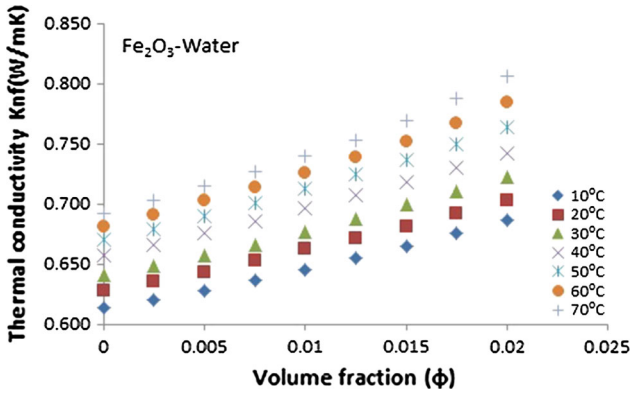

Fig. 7 Thermal conductivity of Fe_2O_3–water nanofluids as a function of volume fraction of Fe_2O_3 nanoparticles at different temperatures

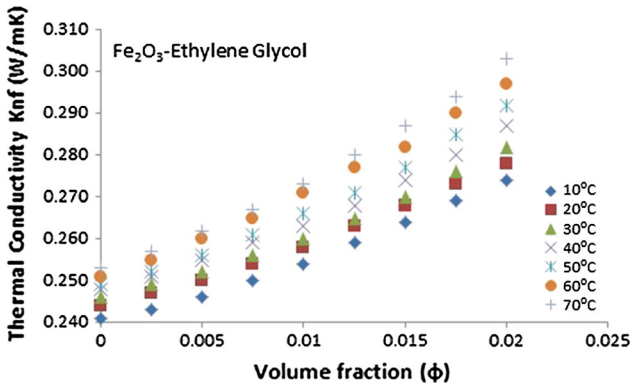

Fig. 8 Thermal conductivity of Fe_2O_3–ethylene glycol nanofluids as a function of volume fraction of Fe_2O_3 nanoparticles at different temperatures

solid (Ref 29). The thermal conductivity of the bridge is not known yet expected to have higher than that of the bulk liquid.

For 0.0025-0.02 volume fraction of Fe_2O_3 nanoparticles in water, thermal conductivity enhances 1.14-11.89 and 1.59-16.45% at 10 and 70 °C, respectively. For the same increase in the volume fraction of Fe_2O_3 nanoparticles in ethylene glycol, thermal conductivity enhances 0.83-13.69 and 1.58-19.76% at 10 and 70 °C, respectively. Though the thermal conductivity of water is higher than ethylene glycol, thermal conductivity enhancement of the Fe_2O_3–ethylene glycol nanofluids is higher

than that of the Fe_2O_3–water nanofluids. Enhancement in thermal conductivity is due to the formation and strengthening of layer-like structure (Ref 28) which is directly dependent on the interaction between nanoparticles and fluids. This diverse interaction may be attributed as the reason for the varying rate of thermal conductivity enhancement for the two base fluids. Results of the study are similar to the work performed by Kumar et al. (Ref 30). Kumar et al. studied Fe_2O_3/water and Fe_2O_3/ethylene glycol nanofluids heat transfer enhancement in a shell and tube heat exchanger. They reported increased thermal conductivity with the increase in concentration. It was suggested that suspended nanoparticles increase turbulence in fluids accelerating energy exchange process. Table 2 summarizes similar prior works, and their results have been compared with the findings of the present study.

3.3 Comparison Between Results of Experimental Measurements, Theoretical Models and ANN Predictions

In the present study, results of experimental measurements have been compared with predictions of standard theoretical models and ANN. Figure 9 and 10 show the comparisons of experimental results of thermal conductivity measurements as a function of volume fraction at 30 °C with predictions of theoretical models and ANN, for Fe_2O_3–water and Fe_2O_3–ethylene glycol nanofluids. ANN predictions are very close to experimental results. Maxwell model, Bruggeman model and Yu and Choi model underestimate the thermal conductivity, while H–C model predictions lie in the middle of estimations by Yu and Choi and ANN. Mean errors in predictions by ANN and H–C model are 0.11 and 1.19% for Fe_2O_3–water nanofluids and 0.17 and 1% for Fe_2O_3–ethylene glycol nanofluids, respectively.

Figure 11 and 12 show the comparisons of experimental results of thermal conductivity measurements as a function of temperature at 0.01 volume fraction with predictions of theoretical models and ANN, for Fe_2O_3–water and Fe_2O_3–ethylene glycol nanofluids, respectively. ANN predictions are well matched with experimental results than predictions by theoretical models. Though the best match with experimental findings, there are disparities with experimental values at $T = 60$ °C (Fig. 11) and $T = 10$ °C (Fig. 12) that may be attributed to overfitting. ANN basically simulates human brains that develop a hypothesis during learning. The learning is affected by sample size, number of features, variance in the aspect values within the feature and between the features, etc. The large variation in the feature values may sometimes affect the performance of the learned system giving rise to such kinds of disparity. Since ANN is a machine learning technique, not the rule-based technique, the disparity may occur randomly or may not occur. Cost of the disparity is generally compared with the overall performance of the learned hypothesis which is quite good in the present case, emphasizing that the disparity can be safely ignored without any significant cost.

The formulations of the used theoretical models do not contain terms for temperature dependency, so the models did not predict thermal conductivity with temperature accurately. Mean errors in predictions by ANN and H–C model are 0.27 and 1.13% for Fe_2O_3–water nanofluids and 0.15 and 0.96% for Fe_2O_3–ethylene glycol nanofluids, respectively.

4. Conclusions

The aim of the present work was to modulate the thermophysical properties of nanofluids for better heat transfer performance. For the purpose, iron oxide nanoparticles have been chosen due to its interesting properties and widespread applicability. The particle size of the synthesized Fe_2O_3 nanoparticles has been in the range of 40-55 nm with a face-

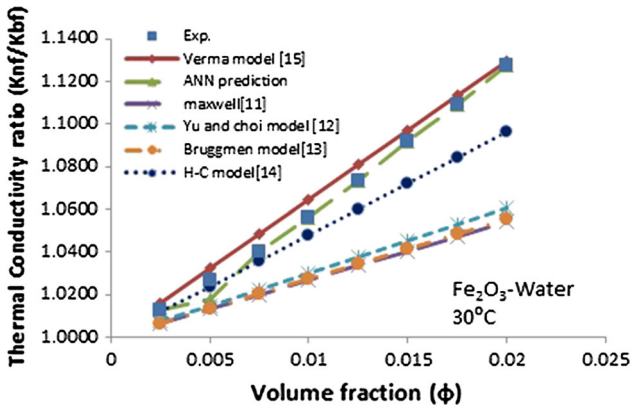

Fig. 9 Comparison of experimental results of Fe_2O_3–water nanofluids' thermal conductivity measurements as a function of volume fraction at 30 °C with predictions of theoretical models and ANN

Table 2 Comparison of our findings with previous works

Reference	Nanoparticles	Size, nm	Base fluids	Concentration range	Temperature range	% increase in thermal conductivity
Kumar et al. (Ref 30)	Fe_2O_3	22	Water	0.02-0.08% volume fraction	30-50 °C	6
Kumar et al. (Ref 30)	Fe_2O_3	22	Ethylene glycol	0.02-0.08% volume fraction	30-50 °C	17
Zouli et al. (Ref 31)	Fe_2O_3	10	Water	0.01-0.09 volume fraction	25-65 °C	32
Guo et al. (Ref 32)	Fe_2O_3	20	Ethylene glycol–deionized water (45:55)	0.005-0.02 volume fraction		3.50
Colla et al. (Ref 33)	Fe_2O_3		Water	5-20 wt.%	10-70 °C	23.65
Huminic et al. (Ref 34)	Fe_2O_3	10	Water	0.5-4 wt.%	20-70 °C	59.00
Nurdin et al. (Ref 35)	Fe_2O_3		Water	0.1-0.6 vol.%	10-35 °C	18.84
Present study	Fe_2O_3	47	Water	0.0025-0.02 volume fraction	10-70 °C	16.45
Present study	Fe_2O_3	47	Ethylene glycol	0.0025-0.02 volume fraction	10-70 °C	19.76

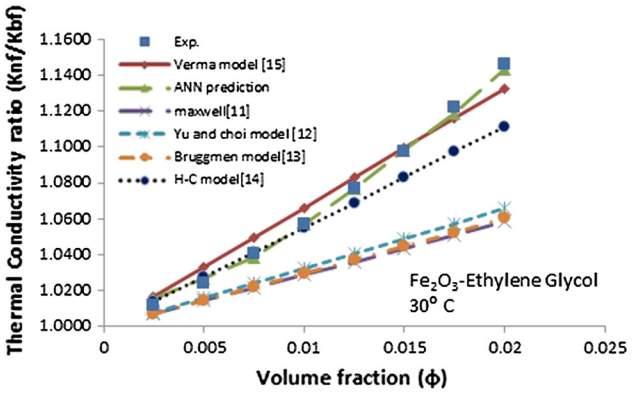

Fig. 10 Comparison of experimental results of Fe_2O_3–ethylene glycol nanofluids' thermal conductivity measurements as a function of volume fraction at 30 °C with predictions of theoretical models and ANN

centered cubic structure having α phase. The thermal conductivity of Fe_2O_3–water and Fe_2O_3–ethylene glycol nanofluids has been higher than that of the base fluids and increases with increasing concentration of dispersed nanoparticles and temperature of the nanofluids. An increase in thermal conductivity with concentration has been higher compared to temperature. At higher concentrations, thermal conductivity enhancement with temperature has been more prominent compared to nanofluids of lower concentrations. For the same concentration of dispersed Fe_2O_3 nanoparticles, the thermal conductivity enhancement rate has been higher for ethylene glycol base nanofluids compared to water base nanofluids.

Estimation using the Maxwell model, the Bruggeman model and the Yu and Choi model exhibits a significant deviation from the experimental results, while the performance of the H–C model is in the acceptable region. Predictions using ANN are very close to experimental results showing significant learning by establishing concentration and temperature dependence of

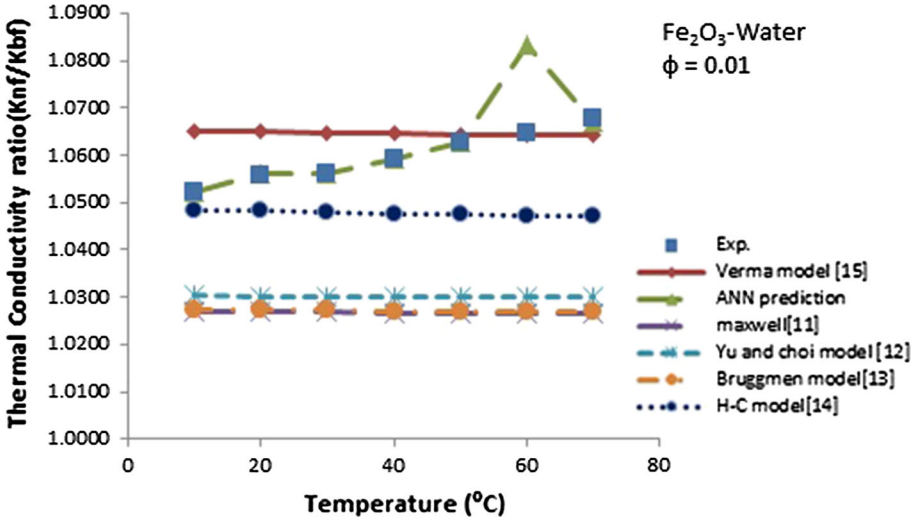

Fig. 11 Comparison of experimental results of Fe_2O_3–water nanofluids' thermal conductivity measurements as a function of temperature at 0.01 volume fraction with predictions of theoretical models and ANN

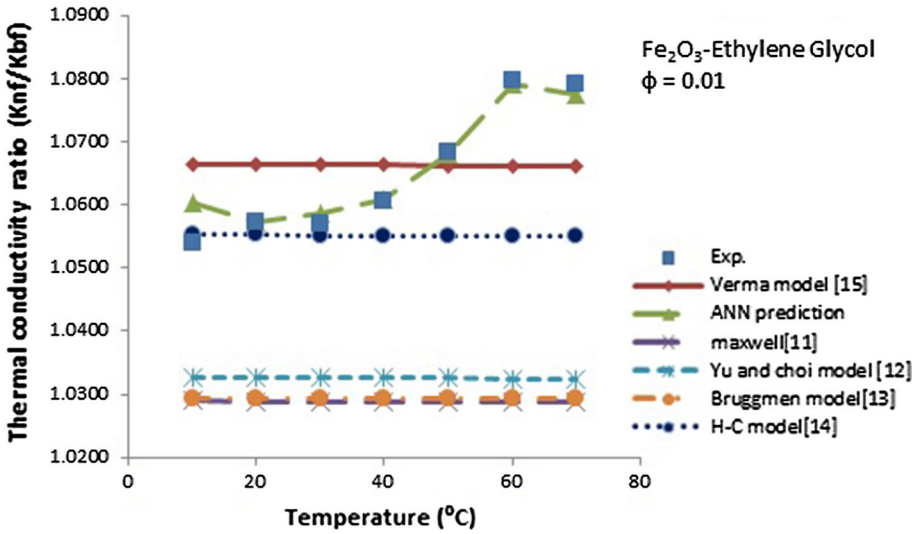

Fig. 12 Comparison of experimental results of Fe_2O_3–ethylene glycol nanofluids' thermal conductivity measurements as a function of temperature at 0.01 volume fraction with predictions of theoretical models and ANN

thermal conductivity. Average percentage errors in prediction using ANN and H–C model are 0.11 and 1.19% for Fe_2O_3–water nanofluids and 0.17 and 1% for Fe_2O_3–ethylene glycol nanofluids, respectively.

The overall findings of the current investigation signify the favorable applicability of Fe_2O_3 nanofluids for heat transfer enhancement. Results emphasize the selection of suitable base fluid as the rate of thermal conductivity enhancement is highly sensitive to base fluid, concentration and temperature. Inline findings of ANN provide an accurate, fast and low-cost alternative to the experimental approach.

Acknowledgments

Research Associateship by Council of Scientific and Industrial Research (CSIR) to Ravi Agarwal and Senior Research Fellowship by University Grant Commission (conducted by Council of Scientific and Industrial Research) to Kamalesh Verma are gratefully acknowledged. Authors are also thankful to the UR-DBT-IPLS (BUILDER) of Centre for Converging Technologies, University of Rajasthan, for allowing using their facilities. KD2 Thermal Properties Analyzer provided by Dr. R. K. Duchaniya (Department of Metallurgical and Material Engineering, Malaviya National Institute of Technology (MNIT), Jaipur, Rajasthan) is also gratefully acknowledged. We thank Keiron O'Shea from Aberystwyth University, UK, for improving the language of the manuscript.

References

1. T.K. Hong, H.S. Yang, and C.J. Choi, Study of the Enhanced Thermal Conductivity of Fe Nanofluids, *J. Appl. Phys.*, 2005, **97**(6), p 1–4
2. K. Hong, T.K. Hong, and H.S. Yang, Thermal Conductivity of Fe Nanofluids Depending on the Cluster Size of Nanoparticles, *Appl. Phys. Lett.*, 2006, **88**(3), p 31901
3. H.E. Patel, S.K. Das, T. Sundararagan, A.S. Nair, B. Geoge, and T. Pradeep, Thermal Conductivities of Naked and Monolayer Protected Metal Nanoparticles Based Nanofluids: Manifestation of Anomalous Enhancement and Chemical Effects, *Appl. Phys. Lett.*, 2003, **83**, p 2931–2933
4. J.A. Eastman, S.U.S. Choi, S. Li, W. Yu, and L.J. Thompson, Anomalously Increased Effective Thermal Conductivities of Ethylene Glycol-Based Nanofluids Containing Copper Nanoparticles, *Appl. Phys. Lett.*, 2001, **78**(6), p 718–720
5. X. Wang, X. Xu, and S.U.S. Choi, Thermal Conductivity of Nanoparticle-Fluid Mixture, *J. Thermophys. Heat Transf.*, 1999, **13**(4), p 474–480
6. H. Masuda, A. Ebata, K. Teramae, and N. Hishinuma, Alteration of Thermal Conductivity and Viscosity of Liquid by Dispersing Ultra-Fine Particles (Dispersion of 7-Al_2O_3, SiO_2, and TiO_2 Ultra-Fine Particles), *Netsu Bus-Sei (Japan)*, 1993, **7**(4), p 227–233
7. S. Lee, S.U.S. Choi, S. Li, and J.A. Eastman, Measuring thermal conductivity of fluids containing oxide nanoparticles, *J. Heat Transf.*, 1999, **121**, p 280–289
8. S.M.S. Murshed, K.C. Leong, and C. Yang, Enhanced Thermal Conductivity of TiO_2—Water Based Nanofluids, *Int. J. Therm. Sci.*, 2005, **44**(4), p 367–373
9. S. Iijima, Helical Microtubules of Graphitic Carbon, *Nature*, 1991, **354**(6348), p 56–57
10. M.S. Liu, M. Ching, L. Cheng, I.T. Huang, and C.C. Wang, Enhancement of Thermal Conductivity with Carbon Nanotube for Nanofluids, *Int. Commun. Heat Mass*, 2005, **32**(9), p 1202–1210
11. J.C. Maxwell, *A Treatise on Electricity and Magnetism, 3rd ed*, Vol 435, Claredon Press, Oxford, 1904
12. W. Yu and S.U.S. Choi, The Role of Interfacial Layers in the Enhanced Thermal Conductivity of Nanofluids, a Renovated Maxwell Model, *J. Nanopart. Res.*, 2003, **5**, p 167–171
13. D.A.G. Bruggeman, Berechnung Verschiedener Physikalischer Konstanten von Heterogenen Substanzen I. Dielektrizitatskonstanten and Leitfanigkeitender Mischkorper aus isotropen Substanzen, *Ann. Phys.*, 1935, **24**, p 636–679
14. R.L. Hamilton and O.K. Crosser, Thermal Conductivity of Heterogeneous Two Component Systems, *Ind. Eng. Chem. Fundam.*, 1962, **1**(3), p 187–191
15. K. Verma, S. Kumar, A. Upadhyay, and R. Singh, Prediction of Thermal Conductivity of Nanofluids Containing Metal Oxide Nanoparticles, *Adv. Sci. Eng. Med.*, 2015, **7**, p 378–384
16. Y. Xuan, Q. Li, and W. Hu, Aggregation Structure and Thermal Conductivity of Nanofluids, *AIChE J.*, 2003, **49**, p 1038–1043
17. J. Koo and C. Kleinstreuer, A New Thermal Conductivity Model for Nanofluids, *J. Nanopart. Res.*, 2004, **6**, p 577–588
18. K. Verma, M. Dabas, A. Upadhyay, and R. Singh, Effective Thermal Conductivity of Lithium Multipurpose Grease Filled with Metal Particles, *J. Reinf. Plast. Compos.*, 2014, **33**(19), p 1794–1801
19. H. Kurt and M. Kayfeci, Prediction of Thermal Conductivity of Ethylene Glycol-Water Solutions by Using Artificial Neural Networks, *Appl. Energy*, 2006, **86**, p 2244–2248
20. J.Z. Liang and G.S. Liu, A New Heat Transfer Model of Inorganic Particulate-Filled Polymer Composites, *J. Mater. Sci.*, 2009, **44**, p 4715–4720
21. R. Agarwal, K. Verma, N.K. Agrawal, R.K. Duchaniya, and R. Singh, Synthesis, Characterization, Thermal Conductivity and Sensitivity of CuO Nanofluids, *Appl. Therm. Eng.*, 2016, **102**, p 1024–1036
22. G. Huminic, A. Huminic, F. Dumitrache, C. Fleaca, and I. Morjan, Experimental Study of Thermo-Physical Properties of Nanofluids Based on γ-Fe_2O_3 Nanoparticles for Heat Transfer Applications, *Heat Transfer Eng.*, 2017, **38**(17), p 1496–1505
23. R. Agarwal, K. Verma, N.K. Agrawal, and R. Singh, Sensitivity of Thermal Conductivity for Al_2O_3 Nanofluids, *Exp. Thermal Fluid Sci.*, 2017, **80**(1), p 19–26
24. S.Z. Guo, Y. Li, J.S. Jiang, and H.Q. Xie, Nanofluids Containing γ-Fe_2O_3 Nanoparticles and Their Heat Transfer Enhancements, *Nanoscale Res. Lett.*, 2010, **5**(7), p 1222
25. E. Ahmadloo and S. Azizi, Prediction of Thermal Conductivity of Various Nanofluids Using Artificial Neural Network, *Int. Commun. Heat Mass Transf.*, 2016, **74**(1), p 69–75
26. L. Motte, What are the Current Advances Regarding Iron Oxide Nanoparticles for Nanomedicine?, *J. Bioanal. Biomed.*, 2012, **4**(6), p 1–2
27. C. Montferrand, Y. Lalatonne, D. Bonnin, L. Motte, and P. Monod, Non Linear Magnetic Behavior Around Zero Field of an Assembly of Superparamagnetic Nanoparticles, *Analyst*, 2012, **137**(1), p 2304–2308
28. W. Yu and S.U.S. Choi, The Role of Interfacial Layers in the Enhanced Thermal Conductivity of Nanofluids: A Renovated Maxwell Model, *J. Nanopart. Res.*, 2003, **5**(1), p 167–171
29. C.J. Yu, A.G. Richter, A. Datta, M.K. Durbin, and P. Dutta, Molecular Layering in a Liquid on a Solid Substrate: An X-ray Reflectivity Study, *Phys. B*, 2000, **283**(1), p 27–31
30. N. Kumar and S.S. Sonawane, Experimental Study of Fe_2O_3/Water and Fe_2O_3/Ethylene Glycol Nanofluid Heat Transfer Enhancement in a Shell and Tube Heat Exchanger, *Int. Commun. Heat Mass*, 2016, **78**(1), p 277–284
31. N. Zouli, I.A. Said, and M. Al-Dahhan, Enhancement of Thermal Conductivity and Local Heat Transfer Coefficients Using Fe_2O_3/Water Nanofluid for Improved Thermal Desalination Processes, *J. Nanofluids*, 2019, **8**(5), p 1103–1122
32. S.Z. Guo, Y. Li, J.S. Jiang, and H.Q. Xie, Nanofluids Containing γ-Fe_2O_3 Nanoparticles and Their Heat Transfer Enhancements, *Nanoscale Res. Lett.*, 2010, **5**(1), p 1222–1227
33. L. Colla, L. Fedele, M. Scattolini, and S. Bobbo, Water-Based Fe_2O_3 Nanofluid Characterization: Thermal Conductivity and Viscosity Measurements and Correlation, *Adv. Mech. Eng.*, 2012, **4**(1), p 1–8
34. G. Huminic, A. Huminic, F. Dumitrache, C. Fleaca, and I. Morjan, Experimental Study of Thermo-Physical Properties of Nanofluids Based on γ- Fe_2O_3 Nanoparticles for Heat Transfer Applications, *Heat Transf. Eng.*, 2017, **38**(17), p 1496–1505
35. I. Nurdin, M.R. Johan, and B.C. Ang, Experimental Investigation on Thermal Conductivity and Viscosity of Maghemite (γ–Fe_2O_3) Water-based Nanofluids, *IOP Conf. Ser. Mater. Sci. Eng.*, 2018, **334**(1), p 1–7